Architecture of the sperm whale forehead facilitates ramming combat

Olga Panagiotopoulou, Panagiotis Spyridis, Hyab Mehari Abraha, David R Carrier, Todd Pataky

Herman Melville's novel Moby Dick was inspired by historical instances in which large sperm whales (Physeter macrocephalus L.) sank 19th century whaling ships by ramming them with their foreheads. The immense forehead of sperm whales is possibly the largest, and one of the strangest, anatomical structures in the animal kingdom. It contains two large oil-filled compartments, known as the "spermaceti organ" and "junk", that constitute up to one-quarter of body mass and extend one-third of the total length of the whale. Recognized as playing an important role in echolocation, previous studies have also attributed the complex structural configuration of the spermaceti organ and junk to acoustic sexual selection, acoustic prey debilitation, buoyancy control, and aggressive ramming. Of these additional suggested functions, ramming remains the most controversial, and the potential mechanical roles of the structural components of the spermaceti organ and junk in ramming remain untested. Here we explore the aggressive ramming hypothesis using a novel combination of structural engineering principles and probabilistic simulation to determine if the unique structure of the junk significantly reduces stress in the skull during quasi-static impact. Our analyses indicate that the connective tissue partitions within the junk reduce stress across the skull during impact; stress reduction is greatest in the anterior aspect of the skull; and removal of the connective tissue partitions increases stress concentrations on the tip of the skull, possibly making it prone to fracture. Although the unique structure of the junk certainly serves multiple functions, our results are consistent with the hypothesis that the structure also evolved to function as a massive battering ram during male-male competition.

1 **Title: Architecture of the sperm whale forehead facilitates ramming combat**

2

3 **Authors:** Olga Panagiotopoulou[1][*], Panagiotis Spyridis[2], Hyab Mehari Abraha[1], David R.

4 Carrier[3], Todd Pataky[4]

5 **Affiliations:**

6 [1] Moving Morphology and Functional Mechanics Laboratory, School of Biomedical Sciences,

7 The University of Queensland, Brisbane 4072, Australia.

8 [2] Polytropos Ltd, London N1 7JL, United Kingdom.

9 [3] Department of Biology, University of Utah, Salt Lake City, UT 84112, USA.

10 [4] Department of Bioengineering, Shinshu University, Ueda, Nagano 386-8567, Japan.

11

12 *Correspondence to:

13 Dr. Olga Panagiotopoulou

14 Moving Morphology and Functional Mechanics Laboratory, School of Biomedical Sciences, The

15 University of Queensland, Room 433-Otto Hirschfeld Building (81), Brisbane, QLD 4072,

16 Australia.

17 o.panagiotopoulou@uq.edu.au

18

19

20

21

22

23

24

25

26

27

28

29

30

31

Peer_J Preprints

32   **Abstract**

33   Herman Melville's novel *Moby Dick* was inspired by historical instances in which large

34   sperm whales (*Physeter macrocephalus L.*) sank 19th century whaling ships by ramming them

35   with their foreheads. The immense forehead of sperm whales is possibly the largest, and one of

36   the strangest, anatomical structures in the animal kingdom. It contains two large oil-filled

37   compartments, known as the "spermaceti organ" and "junk", that constitute up to one-quarter of

38   body mass and extend one-third of the total length of the whale. Recognized as playing an

39   important role in echolocation, previous studies have also attributed the complex structural

40   configuration of the spermaceti organ and junk to acoustic sexual selection, acoustic prey

41   debilitation, buoyancy control, and aggressive ramming. Of these additional suggested functions,

42   ramming remains the most controversial, and the potential mechanical roles of the structural

43   components of the spermaceti organ and junk in ramming remain untested. Here we explore the

44   aggressive ramming hypothesis using a novel combination of structural engineering principles

45   and probabilistic simulation to determine if the unique structure of the junk significantly reduces

46   stress in the skull during quasi-static impact. Our analyses indicate that the connective tissue

47   partitions within the junk reduce stress across the skull during impact; stress reduction is greatest

48   in the anterior aspect of the skull; and removal of the connective tissue partitions increases stress

49   concentrations on the tip of the skull, possibly making it prone to fracture. Although the unique

50   structure of the junk certainly serves multiple functions, our results are consistent with the

51   hypothesis that the structure also evolved to function as a massive battering ram during male-

52   male competition.

53

54

55

56

57

58

59

60

61

62

Introduction

64

65   The sperm whale (*Physeter macrocephalus L.*) is unique in having a massively expanded

66 forehead that is highly sexually dimorphic, being much larger and extending up to a meter and a

67 half beyond the anterior tip of the jaws in mature males (Benzin, 1972; Cranford, 1999).

68 Internally the forehead is composed of two large oil-filled sacs, stacked one on top of the other,

69 known as the spermaceti organ and junk (Fig. 1). These sacs extend for one-third of the total

70 length of the whale and can constitute more than one-quarter of the whale's mass (Benzin, 1972;

71 Clarke, 1978). The oil contained in the upper sac (spermaceti organ) was a primary target of the

72 whaling industry of the early 19th century. At the same time, the forehead of sperm whales was

73 considered by whalers to be a battering ram that the whales sometimes used to attack and sink

74 oak whaling ships of up to 238 tons (Chase, 1821; Starbuck, 1878; Philbrick, 2000).

75   The lower sac (junk) is derived from the ondocete melon (Heyning & Mead, 1990) and is

76 organized into sections by transverse partitions of connective tissue that contain waxy oil

77 (Clarke, 1978) (Fig. 1). The connective tissue partitions are widest about 10-25% of the length

78 from the anterior end and the sections are narrow ventrally and broad dorsally (Clarke, 1978).

79 The partitions become thinner progressively towards the posterior aspect of the junk until they

80 are totally replaced by a mixture of oil and wax. The oil and connective tissue partitions of the

81 junk are enclosed in a fibrous connective tissue case which sits in a trough formed by the upper

82 jaw (Clarke, 1978).

83   The function of the spermaceti organ and junk in adding directionality and amplitude to

84 sonar clicks is relatively well studied and accepted (Møhl et al., 2000; Møhl, 2001; Møhl et al.,

85 2003a; Møhl et al., 2003b; Huggenberger, André & Oelschläger, 2014). Previous studies have

86 also suggested that the unique structural configuration of the sperm whale forehead is

87 functionally related to, acoustic sexual selection (Cranford, 1999), acoustic prey debilitation

88 (Norris & Møhl, 1972), communication (Madsen, Wahlberg & Møhl, 2002) and buoyancy

89 control (Clarke, 1970). Although all of these functional hypotheses are plausible, they cannot

90 explain how the forehead of sperm whales can function as a battering ram capable of sinking

91 ships that are four to five times the mass of the whale.

92   The ramming hypothesis was originally proposed by whalers following the sinking of at

93 least 2 whaling ships, *the Essex* in 1821 and *the Ann Alexander* in 1851 (Chase, 1821; Starbuck,

1878; Philbrick, 2000; Sawtell, 1962). Based on these incidents, researchers have recently suggested that the forehead of a swimming sperm whale possess sufficient momentum to injure an opponent when used as a battering ram, and may at the same time absorb energy to protect the brain and skull of the attacking whale allowing mature males to use their foreheads as battering rams in male-male contests over harems of females (Carrier, Deban & Otterstrom, 2002).

The ramming hypothesis remains highly controversial because (1) the structures that generate sound, the distal sac and monkey lips of the right nasal passage, are located at the rostral end of spermaceti organ (Fig. 1) and are therefore assumed to be in harm's way in a ramming event (Huggenberger, André & Oelschläger, 2014), and (2) ramming episodes have not been observed by scientists who study the behavior of sperm whales. Although the monkey lips do reside at the front end of the spermaceti organ, these structures are located well above and to the right of the rostral end of the junk (Huggenberger, André & Oelschläger, 2014), and it is the junk, not the spermaceti organ, that has been suggested to function as a battering ram during aggressive encounters (Chase, 1821; Carrier, Deban & Otterstrom, 2002). As far as we know, the scientific literature does not include observations of sperm whale ramming behavior, yet there is one documented observation of male-male ramming that we report here (Supplementary Material). On January 30, 1997, a reputable marine biologist, while flying over the Gulf of California, watched two mature males swim directly toward each other, from an initial observed distance of approximately 6.4 kilometers, at an estimated average swimming speed of 17 km/h and collide forehead-to-forehead. Shortly before impact both whales, which had been swimming at the surface, "shallow dove" so that the impact occurred below the surface of the water. This ramming event occurred a few miles north of a group of approximately of 50 females. This observation plus reports of ramming attacks on 19th century whaling ships suggest that sperm whales do sometimes engage in ramming contests. If these ramming contests generally occur at a shallow depth, they may be much more common than whale biologists realize because a human observer would have to be located well above the surface of the water to watch it happen.

Another reason to consider the ramming hypothesis is the extreme body size sexual dimorphism of sperm whales. This species is the most sexually dimorphic of all cetaceans, with mature males being 3-times bigger than mature females (Whitehead, 2003). Among mammals, body size sexual dimorphism is generally greatest in polygynous species in which males compete through fighting and the threat of fighting (Clutton-Brock & Harvey, 1977; Parker, 1983;

4

125   Andersson, 1994). Additionally, because sexual dimorphism is often greatest in those characters

126   that enhance a male's capacity to dominate other males (Clutton-Brock & Harvey, 1977;

127   Hamilton, 1979; Clutton-Brock, Albon & Harvey, 1980; Parker, 1983; Jarman, 1983; Andersson,

128   1994), the observation that the part of the body that is most dimorphic in sperm whales is the

129   length of the head (Nishiwaki, Ohsumi & Maeda 1963) is consistent with the head being a

130   weapon important to male-male competition.

131   This paper addresses the battering-ram hypothesis using finite element analysis and

132   probabilistic simulation. Our main objective was to determine if the connective tissue partitions

133   of the spermaceti junk have potential to reduce stress in the bones of the skull during ramming

134   impact. We predict that the vertically oriented connective tissue partitions within the junk can

135   dissipate load through tension during posteriorly directed compressive loading of the forehead.

136   Bone stress reduction would be particular important on the anterior aspect of the skull (i.e., upper

137   jaw) that would otherwise be most vulnerable to potential tissue damage.

138

139   **Materials and Methods**

140   Finite element analysis (FEA) is a numerical technique well entrenched in comparative

141   biomechanics as a tool to assess the mechanical architecture of anatomical tissues and to better

142   comprehend the complex interaction of their form–function relationships. Nevertheless, FEA

143   accuracy is dependent on a variety of factors and its reproducibility is often obscured in scientific

144   publications due to both public unavailability of the underlying models and the lack of standard

145   reporting guidelines (Erdemir et al., 2012). To mitigate these problems we here describe our

146   methods in accordance with biomechanical FEA reporting guidelines (Erdemir et al., 2012) and

147   we also make all raw data and FE models available for public use (Panagiotopoulou et al. 2015).

148   **Model Identification.** Our study utilized three FE models to study the effect of the connective

149   tissue partitions on the reduction of bone stresses in quasi-static loading of the sperm whale head

150   (Fig. 2).

151   **Model name.** Sperm Whale Head Model A (Generic Base) consisted of twelve connective tissue

152   partitions embedded in the spermaceti tissue of junk.

153   Sperm Whale Head Model B (Half Partitions) had reduced number (six) of connective tissue

154   partitions.

155   Sperm Whale Head Model C (No Partitions) had no connective tissue partitions.

5

156   **Model keywords.** Sperm whale skull, quasi-static impact.

157   **Version.** 0.1 (unpublished).

158   **Physiological domain.** No segmental motion, evenly distributed anterior surface loading, small

159   deformations of hard and soft tissue.

160   **Mechanical domain.** All models were static and linear elastic.

161   **Structure of interest.** The biological structure under investigation was the sperm whale upper

162   jaw (skull).

163   **Demographics.** Adult male sperm whale (*Physeter macrocephalus L.*).

164   **State of represented organism.** *in vitro.*

165   **Disease state.** Healthy.

166   **Spatial scale.** Within a volume of (length 5.3 m x height 1.6 m x width 0.1 m).

167   **Time scale.** Not applicable (quasi-static analysis).

168   **Primary utility**. To provide mechanical insight into a physiologic process.

169   **Secondary utility.** First model of sperm whale skull mechanics.

170   **Primary highlight.** To elucidate the likely mechanically protective role of the vertical

171   connective tissue partitions within the sperm whale skull.

172   **Secondary highlight.** Not applicable.

173   **Primary limitation**. Linear isotropic and homogeneous materials.

174   Due to lack of experimental data on the elasticity of the sperm whale head tissues,

175   anisotropy and heterogeneity, as well as environmental and time dependencies could not be

176   modeled in this study. Thus, isotropy, homogeneity and linear elasticity were assumed and the

177   material properties assigned to each tissue were the closest estimations based on published

178   values of tissues similar to those of interest (Rho, Ashman & Turner 1993; Shahar et al., 2007).

179   A biologically unrealistic consequence of this assumption was that the dorsal horizontal

180   components of connective tissue partitions provided resistance to compression in the model. To

181   this end we assigned a Young's modulus (E) value of 14.8 GPa and Poisson (v) value of 0.1 for

182   the skull; E = 2 GPa and v = 0.2 for the connective tissue partitions; and E = 1 GPa and v = 0.49

183   for the oil/wax mixture enclosed within the spermaceti organ and junk (Fig.2) (Rho, Ashman &

184   Turner 1993; Shahar et al., 2007). Nevertheless, our study was comparative and such an

185   assumption likely created a constant error across all models. Additionally, uncertainties due to

186   material variations had been handled through numerical statistic elaboration of the models.

6

187   Lastly, the basic mechanism of skull-stress reduction we described was independent of model

188   realism.

189   **Secondary limitation**. Simplifications in the model geometry (see below), static simulation.

190   **Reference to publications**. Clarke (1970, 1978); no explicit mechanical model described.

191   *Model Structure*

192   **Loading and boundary conditions.** We used a static force of 764 kN (Fig. 3) distributed evenly

193   over the most anterior aspect of the head as a simplified model of ramming force. We calculated

194   the applied force by assuming that each of the two colliding whales were traveling at an

195   intermediate speed of 6.26 ms^{-1} (Aoki et al., 2007) had masses of 39,000 kg, and decelerated over

196   a distance of 1 meter upon impact. The deceleration distance was based on the length of the

197   spermaceti junk that extended beyond the tip of the skull. Boundary conditions included no-

198   displacement constraints on all external nodes on the posterior surface of the skull.

199   **Primary output variables.** von Mises Stress.

200   **Source of anatomy.** To test our hypothesis, we developed FE models based partially on

201   previously published structural properties and schematic configurations of male sperm whale

202   adult cadavers. Due to the inaccessibility of sperm whale cadaveric species the report by Clarke

203   1978 was the most detailed hitherto available and encompassed skeletal and soft tissues such as

204   the connective tissue partitions, and the oil cases of the spermaceti case and junk. To calculate

205   the dimensions of the various structural components of the model, we scaled the anatomical

206   elements shown in Figure 1 of Clark (1978) to a total spermaceti organ length of 5m (Clarke

207   1970). For modelling purposes and due to the unclear description of the individual connective

208   tissue partitions thickness, we assumed a universal thickness of 0.05m and 0.150m for all

209   connective tissue partitions and the spermaceti junk compartments between the connective tissue

210   partitions respectively (Fig. 2).

211   Model A, representative of the sperm whale head, consisted of the upper sack or

212   spermaceti organ; the lower sack or spermaceti junk; the connective tissue partitions and their

213   subsequent connective tissue case enclosed in the spermaceti junk and the upper jaw (Fig. 2).

214   We compared Model A against two modified models (Models B and C) to assess the

215   mechanical function of the spermaceti organ (Fig. 2). Model B had fewer connective tissue

216   partitions than Model A. Model C lacked the connective tissue partitions altogether (Fig. 2).

7

217   The skin and the blubber were discarded from the modeling process due to their

218   negligible thickness and stiffness.

219   The FE mesh assembly of all models consisted of solid continuum linear tetrahedral

220   elements (type "C3D4" in the Abaqus Library, Simulia-Dassault Systemes, Waltham, USA).

221   Each model contained approximately 42,000 to 48,000 nodes and 220,000 to 260,000 elements.

222   Model A had 257,542 elements in total (28,009 for the upper jaw; 65,588 for the spermaceti

223   case; 91,272 for the spermaceti junk; and 72,673 for the connective tissue partitions). Model B

224   had 242,509 elements in total (278,96 for the upper jaw; 654,67 for the spermaceti case; 93,482

225   for the spermaceti junk; and 55,664 for the connective tissue partitions). Model C had 227,925

226   elements in total (281,37 for the upper jaw; 65,519 for the spermaceti case; 134,269 for the

227   spermaceti junk. The nominal element size was 50 mm (0.05 m), and the actual elements sizes

228   across the model varied from 15 to 85 mm approximately.

229   **Reference configuration.** The Abaqus default x (cranial-caudal), y (medial-lateral), z (vertical)

230   coordinate system was used**.**

231

232   *Simulation structure*

233   **Name of simulation software.** Abaqus/CAE (Simulia-Dassault Systemes).

234   **Version of simulation software.** 6.12

235   **Solution strategy.** Abaqus/Standard implicit direct static solver. Minimum and maximum

236   increments set to 1.000E-05 and 1 respectively.

237   **Numerical algorithms.** Full Newton default iterations.

238   **Convergence criteria.** Default convergence tolerances of the simulation software were used. We

239   interpreted stress differences amongst our models using a Monte Carlo simulation. A total of

240   1000 Monte Carlo iterations were run for each of the three models, varying the three materials'

241   stiffness values randomly with a standard deviation of 10%, and von Mises stress distributions

242   were stored for each iteration (Supplementary Materials Code). This resulted in a population of

243   1000 random individuals which represented the population of interest, under an assumption of

244   10% error in each of the material parameters. The latter is an essential approach in cases when

245   the assigned material properties are based on generalized published values and not on

246   experimental analysis of the tissues of interest.

8

247 For each population pair (i.e. Model B vs. Model A, Model C vs. Model B and Model C vs.

248 Model A), the following statistic was calculated for each element:

249

250

$$z_i = \frac{(\bar{s_i})_\mathrm{B} - (\bar{s_i})_\mathrm{A}}{\frac{1}{2}[(\sigma_i)_\mathrm{A} + (\sigma_i)_\mathrm{B}]}$$

251

252

253 where i indexes the elements, A and B represent models, $\bar{s_i}$ represents mean elemental von Mises

254 stress and σ_i represents elemental standard deviation. Since the input variance nonlinearly maps

255 to elemental variance, the z distribution is a non-trivial function of mean group differences.

256 Next, the "significance" of the z distribution was assessed using paired non-parametric

257 permutation tests (one for each model pair). A total of 10,000 label permutations were applied to

258 each model pair, yielding a non-parametric distribution of the z statistic at each element. The

259 99th percentile of that distribution was taken as the "significance" threshold. In other words, if

260 an element's z value survived that threshold, it would suggest that 99% of all randomly labelled

261 individuals would yield a z value less than that observed in the original labellings, and thus that

262 threshold-surviving elements represented true population differences at alpha=0.01 under the

263 assumption of 10% true population material parameter variance.

264 ***Validation.*** Validation of the FE models against experimental *ex vivo* data was not feasible due

265 to size and accessibility constraints. Nevertheless our study is comparative and conclusions are

266 fundamentally mechanical rather than empirical.

267 ***Availability.*** Not yet public.

268

269 **Results**

270 In all our FE models the highest concentration of von Mises stresses occurred in the most

271 anterior aspect of the skull (Figs. 4, 5 and Table 1). The anterior connective tissue partitions

272 within the junk were subjected to higher tensile loading than the posterior portions (Fig. 6).

273 Tension in the connective tissue partitions redistributed compressive stresses across the skull

274 (Models A and B) and the absence of the partitions (Model C) raised anterior skull stresses (Fig.

275 4, 5 and Table 1).

276 A reduced number of partitions (Model B) did reduce stresses in the anterior skull, but stress

9

277 reduction was not as effective as Model A (Fig. 4, 5 and Table 1). The skull stress difference

278 distributions resulting from Monte Carlo simulations suggest that our main finding regarding the

279 load-redistribution functionality of the connective tissue is insensitive to relatively large changes

280 in both material parameters (Fig. 7) and, indirectly, load magnitudes.

281

282 **Discussion**

283 Our findings suggest that the connective tissue partitions of the junk may be able to

284 reduce impact stresses and thus potentially function as a protective mechanism during ramming.

285 The mechanism of skull stress reduction appears to be connective partition tension; as the

286 spermaceti junk is compressed upon impact, the oil between the partitions is displayed vertically

287 and laterally, placing the connective tissue partitions into tension (Fig. 6). This connective tissue

288 tension allows the total compressive bone load to be shared over a greater volume (Figs. 4-7).

289 While our static simulations do not quantify dynamic effects of the connective partitions

290 including energy dissipation, our results suggest that connective partition tension would in fact

291 dissipate energy in dynamic impacts because dynamic loading, like the current quasi-static

292 loading, would be distributed over a broader region of the skull. Additionally, during a dynamic

293 impact soft tissues within the skull would displace, and the connective tissue partitions would

294 limit this displacement. The connective tissue might therefore protect both bone and soft tissue

295 from injury. Absence of the partitions increased stresses by 45%, concentrated on the most

296 anterior aspect of the skull, making the skull more prone to tissue failure (Table 1, Figs.4-7).

297 Our findings appear to provide an explanation for previous observations that, in real

298 whales, the partitions become progressively thinner posteriorly until they are replaced by a

299 mixture of oil and wax (Clark, 1978). The anterior thicker partitions are subjected to the greatest

300 tensile loading (Fig. 6) and, if the battering ram hypothesis is correct, they likely play the biggest

301 role in skull stress reduction in the face of posteriorly-directed impact forces.

302 The connective tissue partitions of the junk are acquired traits that likely facilitate a

303 variety of functions. In addition to acoustic signals between groups (Madsen, Wahlberg & Møhl

304 2002), the partitions may play an important role in the dissipation of stresses during ramming

305 combat to protect the skull and brain. This "mechanical advantage" is a trait that is likely related

306 to selection on male-male aggressive behavior. Such developmental non-independent

307 morphological features of the junk are an example of how a derived structure, such as the

10

308 connective tissue partitions, facilitates evolutionary modifications while maintaining functional

309 integrity (Wagner & Altenberg 1996).

310   Our results are not directly relevant to the behavioral strategies behind ramming impacts;

311 however, our findings are consistent with the hypothesis proposed in 1821 by Owen Chase

312 (Chase, 1821). Following the sinking of *the Essex* whaling ship, Owen Chase hypothesized that

313 sperm whales not only use their immense and elaborately complex foreheads as battering rams

314 when fighting, but also that "*the whale's head is admirably designed for this mode of attack*".

315 The prevalence of head-butting in sperm whales is not well documented. However, ramming is a

316 basal behavior for bovidae (Farke, 2008; Alvaraez, 1990) and cetacean (Carrier, Deban &

317 Otterstrom, 2002), including humpback whales (Baker & Herman 1984), bottle-nosed whales

318 (Gowans& Rendell 1999), narwhales (Silverman & Dunbar 1980), long-finned pilot whales

319 (Reilly & Shane, 1986) and killer whales (Goley & Straley, 1994). Based on these reports, it has

320 previously been hypothesized that the spermaceti organ of male sperm whales may function as a

321 weapon and is more developed in males due to sexual selection (Carrier, Deban & Otterstrom,

322 2002). If this is true then males may be exposed to increased stresses during head-butting

323 ramming and as such necessitate additional support via a dramatically increased and more

324 structurally robust melon.

325   Our study illustrates how structural engineering principles and probabilistic simulation

326 can be used to address hypotheses of mechanical function in biological systems that are too big

327 or inaccessible to be studied directly. We anticipate our study will stimulate future research

328 aimed at unraveling the mechanical function of the head during aggressive head-butting and

329 ramming in other species such as the *Hippopotamus* (Kingdon, 1979) which head-butting

330 aggressive behavior is common but remains unsimulated.

331

337

338

References:

Alvarez F. 1990. Horns and fighting in male Spanish ibex, *Capra pyrenaica*. Journal of Mammalogy 71: 608-616.

Andersson M. 1994. *Sexual Selection*. Princeton: Princeton University Press.

Aoki K, Amano M, Sugiyama N, Muramoto H, Suzuki M, Yoshioka M, Mori K, Tokuda D, Miyazaki N. 2007. Measurement of swimming speed in sperm whales. In *Underwater technology and workshop on scientific use of submarine cables and related technologies.* IEEE ,467- 471.

Baker CS, Herman LM. 1984. Aggressive behavior between humpback whales (*Megaptera novaeangliae*) wintering in Hawaiian waters. *Canadian Journal of Zoology* 62: 1922–1937.

Berzin AA. 1972. *The Sperm Whale*. Israel Program for Scientific Translations, Jerusalem.

Carrier RC, Stephen MD, Otterstrom J. 2002. The face that sank the *Essex:* potential function of the spermaceti organ in aggression. *Journal of Experimental Biology* 205: 1755-1763.

Chase O. 1821. *Shipwreck of the Whale-Ship Essex*. New York, Gilley.

Clarke MR. 1970. Function of the spermaceti organ of the sperm whale. *Nature* 228: 873-874.

Clarke MR. 1978. Structure and proportions of the spermaceti organ in the sperm whale. *Journal of the Marine Biology Association* 58: 1-17.

Clutton-Brock TH, Albon SD, Harvey PH. 1980. Antlers, body size and breeding group size in the Cervidae. *Nature* 285: 565–566.

Clutton-Brock TH, Harvey PH. 1977. Primate ecology and social organization. *Journal of Zoology London* 183: 1–39.

12

370

Cranford TW. 1999. The sperm whale's nose: sexual selection on a grand scale? *Marine*

Mammal Science 15: 1133-1157.

373

Erdemir A, Guess TM, Halloran J, Tadepalli SC, Morrison TM. 2012. Considerations for

reporting finite element analysis studies in biomechanics. *Journal of Biomechanics* 45: 625-633.

376

Farke AA. 2008. Frontal sinuses and head-butting in goats: a finite element analysis. *Journal of*

Experimental Biology 211:3085-3094.

379

Goley PD, Straley JM. 1994. Attack on gray whales (*Eschrichtius robustus*) in Monterey Bay,

California by killer whales (*Orcinus orca*) previously identified in Glacier Bay, Alaska.

Canadian Journal of Zoology 72: 1528–1530.

383

Gowans S, Rendell L. 1999. Head-butting in northern bottlenose whales (*Hyperodon*

ampullatus): A possible function for big heads. *Marine Mammal Science* 15: 1342-1350.

386

Hamilton WD 1979. Wingless and fighting males in fig wasps and other insects. In: Blum MS,

Blum NA, eds. *Sexual selection and reproductive competition in insects*. New York, Academic

Press, 167-220.

390

Heyning JE, Mead JG. 1990. Evolution of the nasal anatomy of cetaceans. In: Thomas J,

Kastelein R*,* eds. *Sensory Abilities of Cetaceans.* New York: Plenum Press, 67–79.

393

Huggenberger S, André M, Oelschläger HHA. 2014. The nose of the sperm whale: overviews of

functional design, structural homologies and evolution. *Journal of Marine Biological Association*

of the United Kingdom 1-24. DOI:10.1017/S0025315414001118.

397

Jarman PJ. 1983. Mating system and sexual dimorphism in large, terrestrial, mammalian

herbivores. *Biology Reviews* 58: 485–520.

13

NOT PEER-REVIEWED

400   Kingdon J. 1979. *East African Mammals*, vol. III. London: Academic Press.

401

402   Madsen PT, Wahlberg M, Møhl B. 2002. Male sperm whale (*Physeter macrocephalus*) acoustics

403   in a high-latitude habitat: implications for echolocation and communication. *Behavioural*

404   *Ecology and Sociobiology* 53: 31-41.

405

406   Møhl B, Madsen PT, Wahlberg M, Au WWL, Nachtigall PE, Ridgway SH. 2003a. Sound

407   transmission in the spermaceti complex of a recently expired sperm whale calf. *Acoustics*

408   *Research Letters Online* 4: 19–24.

409

410   Møhl B, Wahlberg M, Madsen PT, Heerfordt A, Lund A. 2003b. The monopulsed nature of

411   sperm whale clicks. *Journal of the Acoustical Society of America* 114: 1143–1154.

412

413   Møhl B, Wahlberg M, Madsen PT, Miller LA, Surlykke A. 2000. Sperm whale clicks:

414   directionality and source level revisited. *Journal of the Acoustical Society of America* 107: 638–

415   648.

416

417   Møhl B. 2001. Sound transmission in the nose of the sperm whale *Physeter catodon*. A post

418   mortem study. *Journal of Comparative Physiology. A, Sensory, Neural, and Behavioral*

419   *Physiology* 187: 335–340.

420

421   Nishiwaki M, Ohsumi S, Maeda Y. 1963. Change of form in the sperm whale accompanied with

422   growth. *Scientific Reports of the Whales Research Institute Tokyo* 17: 1–17.

423

424   Norris KS, Harvey GW. 1972. In: Galler SR, Schmidt-Koenig K, Jacobs GJ, Belleville RE. eds.

425   *Animal orientation and navigation NASA special publication.* Washington: NASA scientific and

426   technical office, 397-417.

427

428   Panagiotopoulou O, Spyridis P, Mehari Abraha H, Carrier DR, Pataky T. 2015. Architecture of

429   the sperm whale forehead facilitates ramming combat. Dryad Digital Repository. http://To be

430   completed after paper acceptance

14

431

432   Parker GA. 1983. Arms races in evolution – an ESS to the opponent independent costs game.

433   *Journal of Theoretical Biol*ogy 101:619–648.

434

435   Philbrick N. 2000. *In The Heart Of The Sea.* Harmondsworth, Penguin Books Ltd.

436

437   Reilly SB, Shane SH. 1986. Pilot whale. In *Marine Mammals of Eastern North Pacific and*

438   *Arctic Waters* (ed. Haley D.) 133–139 (Pacific Search Press, Seattle.

439

440   Rho JY, Ashman RB, Turner CH. 1993. Young's modulus of trabecular and cortical bone

441   material: ultrasonic and microtensile measurements. *Journal of Biomech*anics 26: 111-119.

442

443   Sawtell CC. 1962. *The Ship Ann Alexander of New Bedord, 1805-1851.* Mystic, Marine

444   Historical Association.

445

446   Shahar, R, Zaslansky P, Barak M, Friesem AA, Currey JD, Weiner S. 2007. Anisotropic

447   Poisson's ratio and compression modulus of cortical bone determined by speckle interferometry.

448   *Journal of Biomechanics* 40: 252-264.

449

450   Silverman HB, Dunbar MJ. 1980. Aggressive tusk use by the narwhal (*Monodon monoceros L.*).

451   *Nature* 284: 57–58.

452   Starbuck A. 1878. *History of the American Whale Fishery, From Its Earliest Inception To The*

453   *Year 1876.* New York, Argosy-Antiquarian Ltd.

454

455   Wagner GP, Altenberg L. 1996. Complex adaptations and the evolution of evolvability.

456   *Evolution* 50: 967–976.

457

458   Whitehead H, Weilgart L. 2000. In: Mann J, Connor RC, Tyack PT, Whitehead H. eds. *Cetacean*

459   *Societies, Field Studies of Dolphins and Whales.* Chicago, Univ. Chicago Press, 154-1772

460

15

461 Whitehead H. 2003. *Sperm whales: social evolution in the ocean.* Chicago, University of

462 Chicago Press.

463

464 **Figure legends**

465 **Fig. 1.** Schematic representation of sperm whale head structure.

466 **Fig. 2.** Finite element models. Young's moduli for the connective tissue partitions (blue),

467 spermaceti organ (yellow) and skull (red) were 14.8 GPa, 1 GPa and 2 GPa, respectively. Models

468 A, B and C have twelve, six and zero connective tissue partitions, respectively.
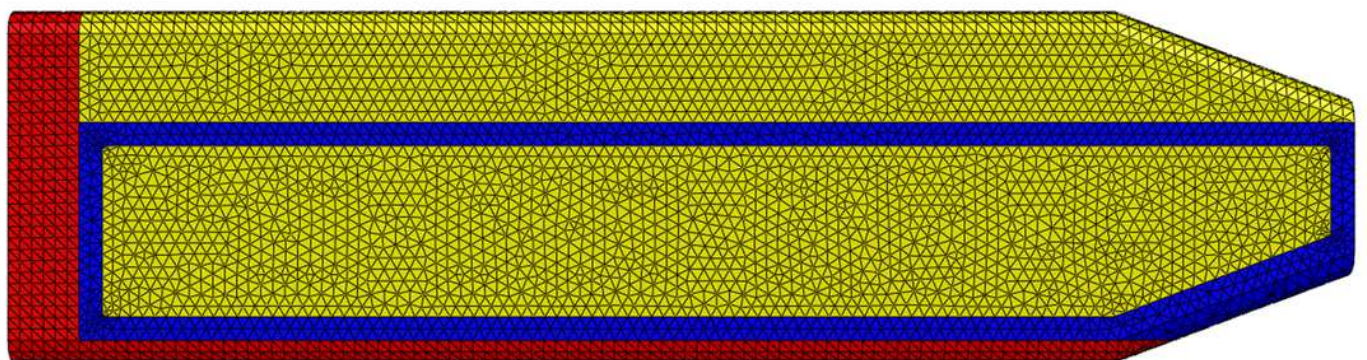
469 **Fig. 3.** Loads and constraints assigned to all FE models. A force of 764 kN was applied to the

470 anterior surface of the head (1). Motion was constrained at the posterior surface (2) in all

471 directions.

472 **Fig. 4.** Von Mises stress distribution results.

473 **Fig. 5**. Region definitions (blue vertical bars).

474 **Fig. 6.** Maximum principal stress distributions across the connective tissue partitions. Positive

475 and negative stresses indicate areas of tension and compression respectively.

476 **Fig. 7.** Z statistic distributions depicting mean elemental von Mises stress differences divided by

477 elemental standard deviation under an assumed population material stiffness variance of 10%.

478 Data are thresholded at alpha=0.01.

479

Table 1(on next page)

Maximum (Max.), mean and minimum (Min.) percentage increase of the regional (Fig. 5) von Mises stress values (Pa) between Models A and C and Models B and C.

Table 1.
Maximum (Max.), mean and minimum (Min.) percentage increase of the regional (Fig. 5) von Mises stress values (Pa) between Models A and C and Models B and C.

	% increase														
	1			2			3			4			5		
	Max.	Mean	Min.	Max.	Mean	Min.	Max.	Mean	Min.	Max.	Mean	Min.	Max.	Mean	Min.
Model A - Model C	42.9	45.7	3.6	25	24.1	9.4	-8.8	6.1	60.8	-6.5	-0.9	-27.3	1.4	-0.3	-62.8
Model B - Model C	10.1	15.5	12.8	-7.3	4.1	35.7	0.6	0.8	-6.9	-6.7	-1.4	-27.4	1.4	-0.2	-59.6

1

Schematic representation of sperm whale head structure.

2
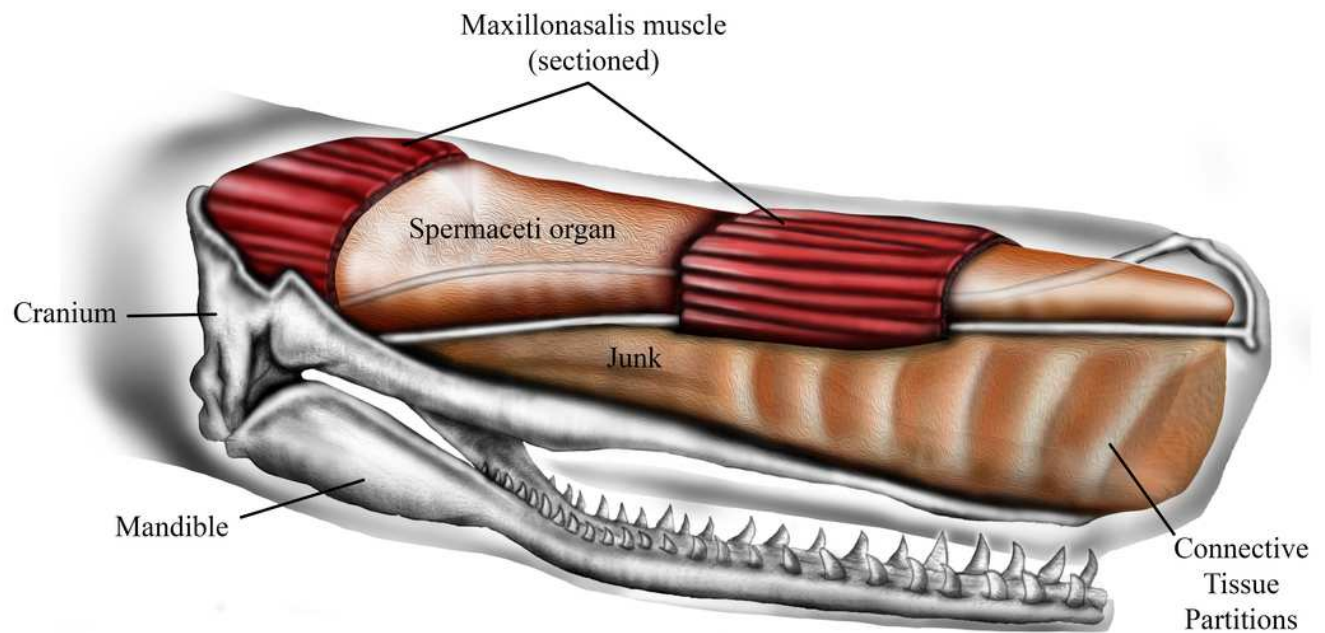
Finite element models.

Young's moduli for the connective tissue partitions (blue), spermaceti organ (yellow) and skull (red) were 14.8 GPa, 1 GPa and 2 GPa, respectively. Models A, B and C have twelve, six and zero connective tissue partitions, respectively.
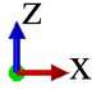
Model A
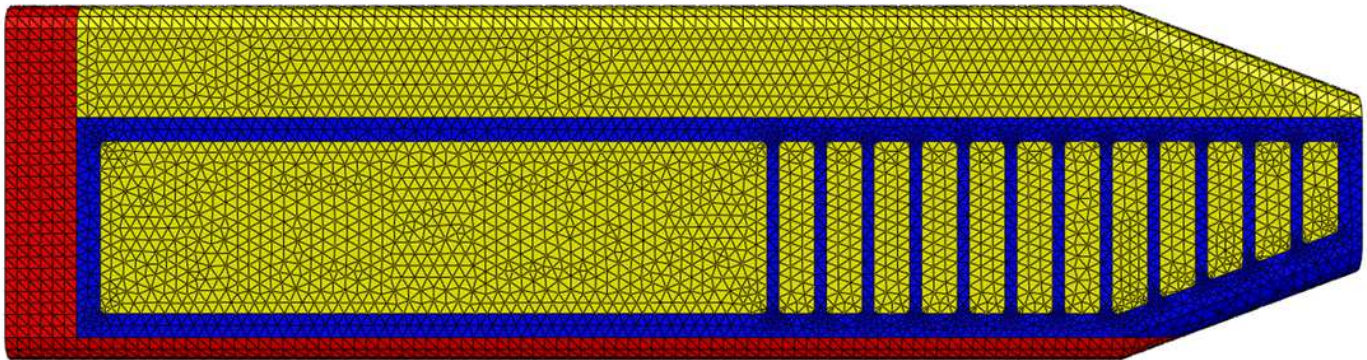
Model B
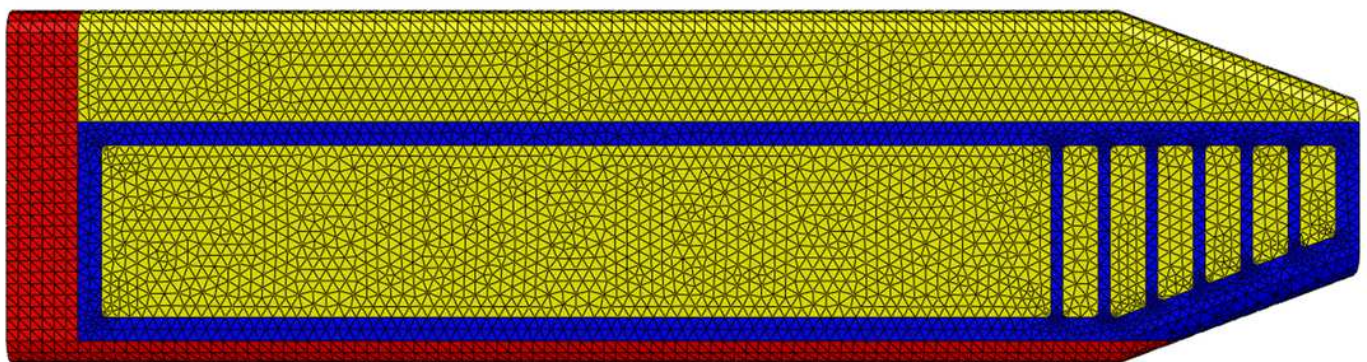
Model C

3

Loads and constraints assigned to all FE models.

A force of 764 kN was applied to the anterior surface of the head (1). Motion was constrained at the posterior surface (2) in all directions.
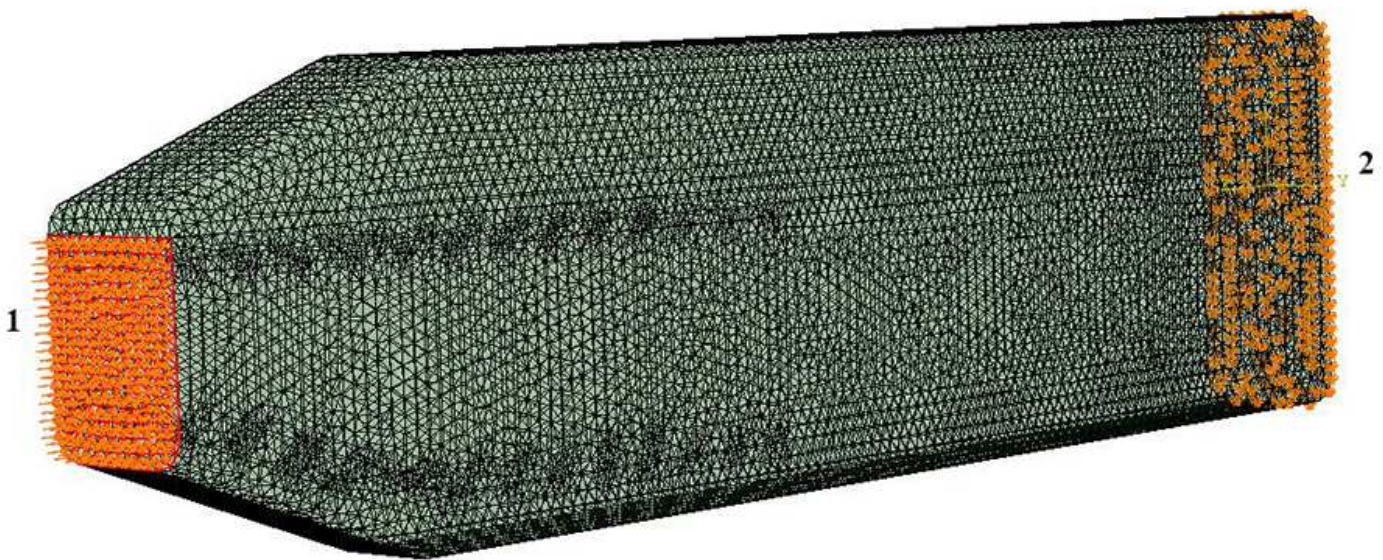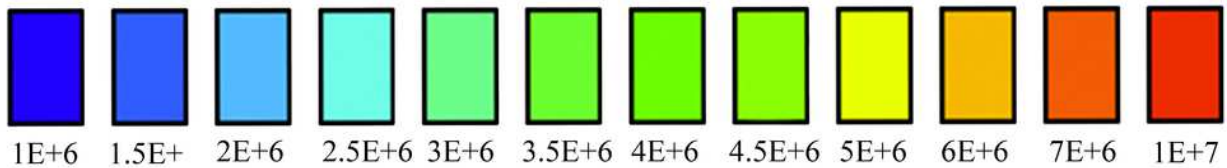
4

Von Mises stress distribution results.
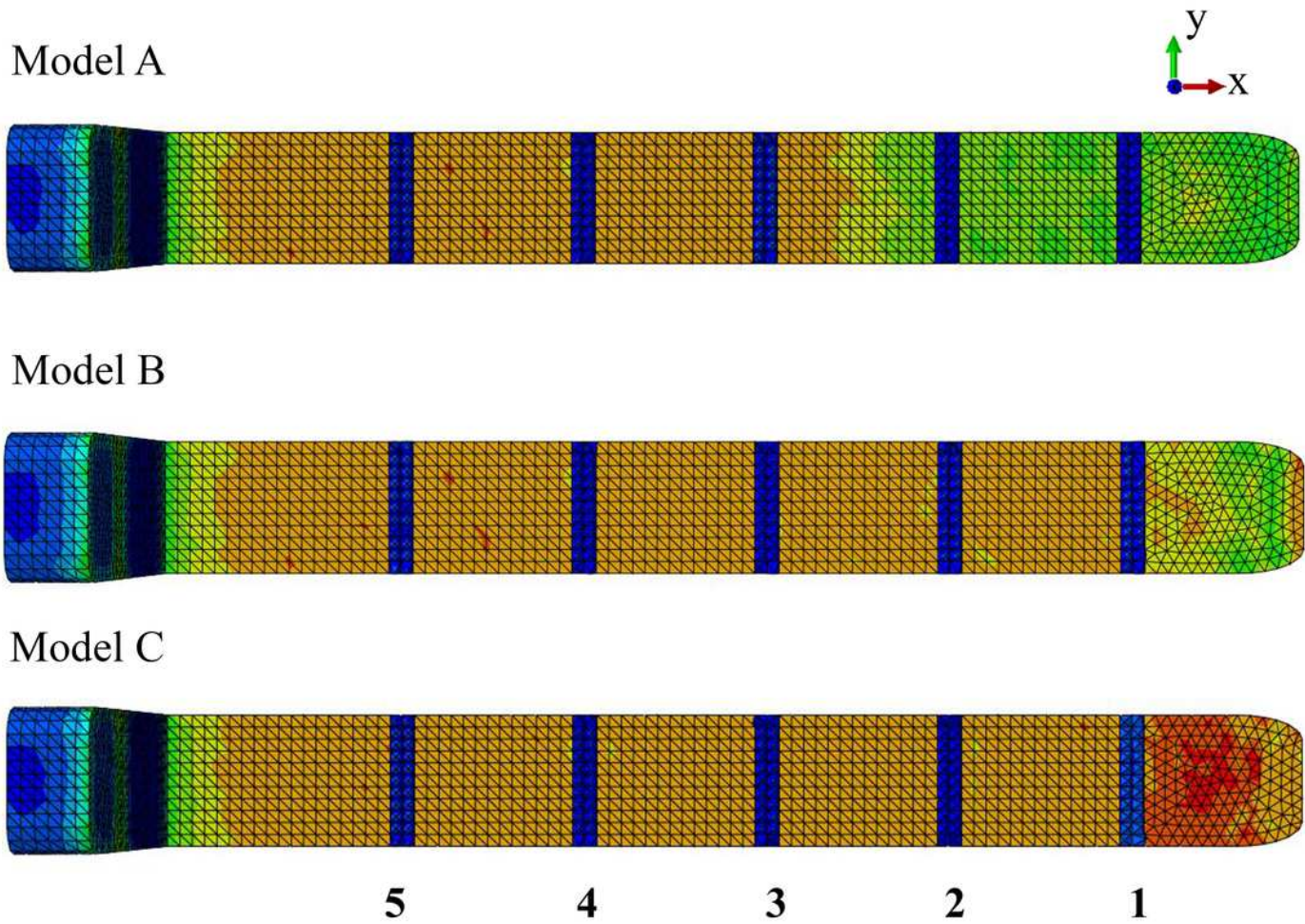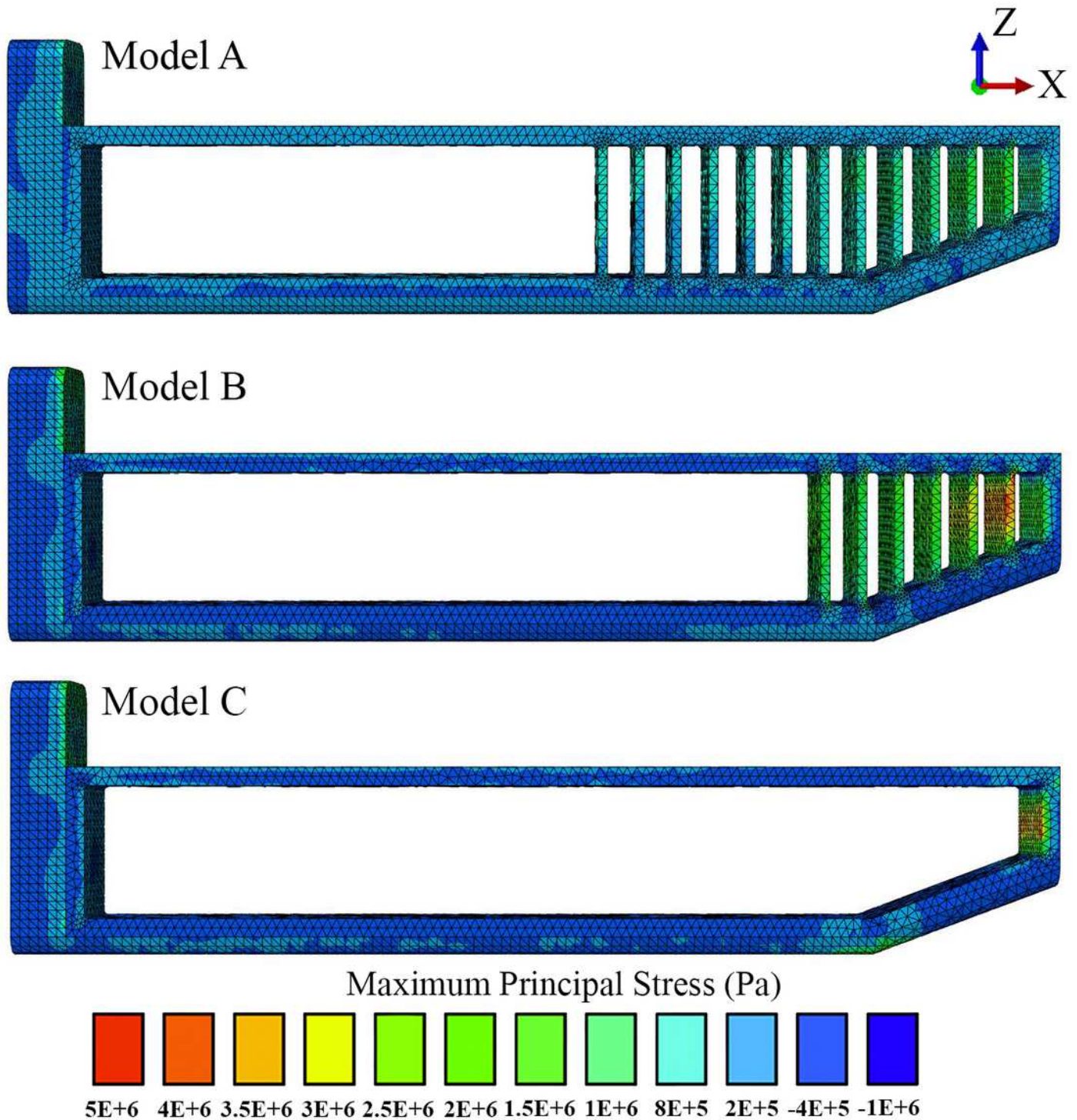
5
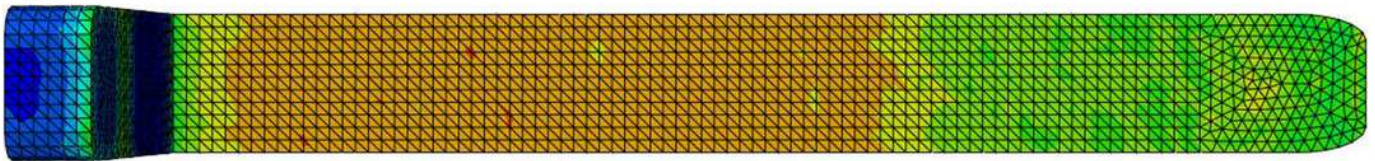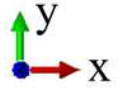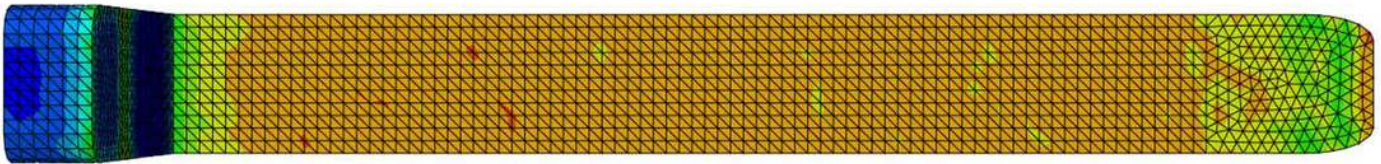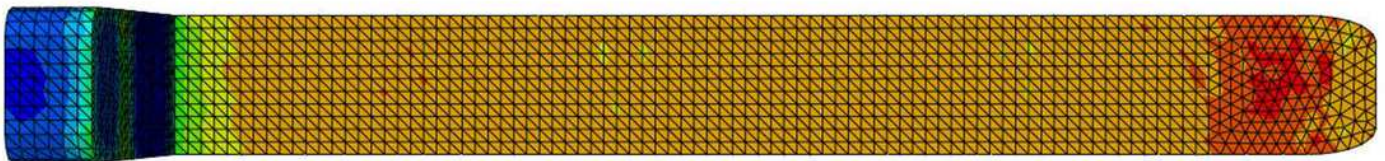
Region definitions (blue vertical bars).

6

Maximum principal stress distributions across the connective tissue partitions.

Positive and negative stresses indicate areas of tension and compression respectively.

Maximum Principal Stress (Pa)

5E+6 4E+6 3.5E+6 3E+6 2.5E+6 2E+6 1.5E+6 1E+6 8E+5 2E+5 -4E+5 -1E+6

7

Probabilistic FEA simulation.

Z statistic distributions depicting mean elemental von Mises stress differences divided by elemental standard deviation under an assumed population material stiffness variance of 10%. Data are thresholded at alpha=0.01.